© [2005] IEEE. Reprinted, with permission, from [Tang Zhongwei; Sanagavarapu Ananda, Experimental Investigation of Indoor MIMO Ricean
Channel Capacity, IEEE ANTENNAS AND WIRELESS PROPAGATION LETTERS, VOL. 4, 2005]. This material is posted here with permission of the IEEE. Such permission of the IEEE does not in any way imply IEEE endorsement of any of the University of Technology, Sydney's products or services. Internal or personal use of this material is permitted. However, permission to reprint/republish this material for advertising or promotional purposes or for creating new collective works for resale or redistribution must be obtained from the IEEE by writing to pubs-permissions@ieee.org. By choosing to view this document, you agree to all provisions of the copyright laws protecting it

Experimental Investigation of Indoor MIMO Ricean Channel Capacity

Zhongwei Tang, *Student Member, IEEE*, and Ananda S. Mohan, *Member, IEEE*

Abstract--We investigate the variation of measured MIMO channel capacity for line-of-sight (LOS) Ricean scenarios inside a typical indoor environment for various transmitter-receiver positions at a centre frequency of 2.45 GHz. In order to quantify the effect of LOS component on indoor MIMO performance, an absorber-loaded metal panel was utilized to artificially obstruct the LOS path between the transmit and receive antennas. Our results confirm that MIMO capacity decreases with the increase in the values of Ricean *K* factor. We have also observed that the variation in channel capacity closely follows the corresponding deviations in root mean square (RMS) delay spread of the channel.

Index Terms— Indoor Ricean channel, MIMO capacity, LOS, Ricean *K* factor, RMS delay spread.

I. Introduction

It has been well established that the channel capacity of multi-input multi-output (MIMO) systems is strongly reliant on the propagation environments [1-3]. The effect of the line-of-sight (LOS) component in Ricean channels on the achievable MIMO capacity was theoretically investigated in [4,5], where it was shown that the ergodic capacity decreases with the increase in the contribution of the LOS component. It is well known that the contribution of LOS component is represented by the Ricean *K* factor. For outdoor Ricean MIMO channels, the effect of LOS component on capacity was investigated in [6]. However, to the best of authors' knowledge, experimental validation of the effect of LOS component in indoor Ricean MIMO channels is not reported so far in the open literature. In this paper, we experimentally investigate the effect of LOS component on indoor MIMO

capacity in a practical indoor environment. We show that in a classroom environment, the indoor MIMO capacity increases with the decrease in the Ricean *K* factor. In addition, our study has indicated that the capacity increases with the increase in the value of the root mean square (RMS) delay spread of the channel.

II. Indoor MIMO Channel Measurements

The indoor MIMO channel measurements were performed inside a typical rectangular-shaped classroom located on the 23rd floor of the 28-storey Tower Building of the University of Technology, Sydney (UTS). The schematic of the classroom is shown in Fig.1. The measurements were performed using a vector network analyzer (VNA) HP 8720A at a centre frequency of 2.45 GHz for vertical polarization inside the classroom. The measurements were conducted during weekends to avoid the movement of people so as to approximate a quasistatic channel condition. Both the transmit and receive arrays were formed as synthetic arrays using commercially available sleeve dipole antennas in order to avoid mutual coupling and also to reduce the complexity and cost of the MIMO measurement. The return loss of the two sleeve dipole antennas was measured to be below -15 dB within the considered bandwidth. To obtain a virtual transmit array, a computer controlled angular scanner moved a sleeve dipole antenna around a circle to form a virtual uniform circular array. At the receiver, the virtual uniform rectangular receive array was obtained using a computer controlled X-Y scanning system to move a dipole antenna over the horizontal plane. For each transmitter-receiver configuration, 801 frequency response measurements were acquired within a bandwidth of 120 MHz.

The classroom, as schematically depicted in Fig.1, has dimensions of 14.95×7.46 m^2 with a height of 3.62 m; contains a number of wooden desks and plastic chairs, and is enclosed by a concrete wall on one side with a wide metal-framed glass window. The other three sides of the room have brick internal walls. The two entrances to the room consist of two wooden

doors, which open into a corridor. In the measurements, with reference to Fig.1, the transmit antenna was fixed at a position, denoted as B, whilst the receiver was moved between different positions, indicated as I, D, G, F and H inside the room. During all the measurements, the heights of both transmit and receive antennas were fixed at 1.7 m above the floor level.

In the measurements, a 4-element uniform circular array with a radius of half a wavelength was formed at the transmitter and a 4-element planar square array with an interelement-spacing of half a wavelength was synthesized at the receiver. At each receiving position, a total of nine 4-element synthetic planar square arrays were formed. Therefore, for each transmitter-receiver pair, a total of 7209 (9×801) spatial and frequency 4×4 MIMO realizations were obtained.

In order to validate the effect of LOS component on Ricean indoor MIMO channel capacity, an absorber-loaded metal panel was utilized in our measurements. The absorber-panel, having dimensions of 1 m×1 m, was used to artificially obstruct the LOS path between the transmit and receive antennas so as to obtain Obstructed LOS (OLOS) channel conditions. Henceforth, in this paper, we refer to LOS scenarios when the absorber-panel was not used in measurements, and refer to OLOS scenarios when the absorber-panel was used.

The MIMO channel capacity is calculated with the uniform power allocation scheme [1]:

$$C = \log_2 \det(I + (\rho / n_t) HH^*) \tag{1}$$

where *det*() is the matrix determinant, n_t is the number of transmit antennas, ρ is the mean receive signal-to-noise ratio (SNR), I is an identity matrix, H^* is the conjugate transpose of the normalized channel transfer matrix H.

To calculate the measured channel capacity, it is necessary that the acquired channel transfer matrices be normalized. We used the Frobenius norm in our calculations, given by:

$$\sum_{i=1}^{n_t}\sum_{j=1}^{n_r}\left|h_{ji}\right|^2 = n_r n_t \tag{2}$$

where h_{ji} is the element of the channel transfer matrix, n_t and n_r are the number of transmit and receive array elements. In our data analysis, we employed two different normalization schemes by using equation (2) for two different purposes. The use of the first normalization scheme is to compare the MIMO performance at the same receive SNR level while disregarding the path loss effect. The use of the second normalization scheme is to evaluate the achievable MIMO capacity whilst accounting for the path loss effect due to the obstruction of LOS path when using the absorber-panel. For the first scheme, the acquired MIMO transfer matrix of each MIMO realization was normalized to satisfy equation (2) to calculate capacity by setting SNR 'ρ' equal to 20 dB. This ensures that for each MIMO realization at each receiving position, ignoring the path loss effect, the receive SNR is the same. For the second normalization scheme, the measured obstructed LOS channel matrices at each receive position are multiplied by a mean normalization constant obtained from the previous step for corresponding LOS case, which satisfy equation (2). Thus, we obtain new matrices to calculate OLOS MIMO capacity by setting SNR 'ρ' equal to 20 dB. In doing this, the actual receive SNR for the obstructed LOS scenario is less than that of its corresponding LOS case which is equal to 20 dB, and hence, the effect of path loss due to the obstruction of LOS path is properly accounted for.

The average power delay profile (PDP) was obtained by applying IFFT on the frequency responses of all single-input single-out channels of a MIMO connection pair. Then, the root mean square delay spread, σ_τ, of this pair was calculated using:

$$\sigma_\tau = \sqrt{\overline{\tau^2} - (\bar{\tau})^2} \tag{3}$$

where $\bar{\tau} = \sum_i \beta_i^2 \tau_i / \sum_i \beta_i^2$ and $\overline{\tau^2} = \sum_i \beta_i^2 \tau_i^2 / \sum_i \beta_i^2$, where β_i is the amplitude at time delay τ_i.

The Ricean *K* factor is defined as the ratio of the fixed to variable power components. We estimate the mean *K* factor for each MIMO connection by using the moment-method [7] on the acquired data that are averaged over all the SISO channels for each position. The *K* factor is calculated as:

$$K = \sqrt{1-\gamma}/(1-\sqrt{1-\gamma}) \tag{4}$$

where $\gamma = \sigma_r^2 / P_r^2$, σ_r is the variance of the receive signal power about its mean P_r.

III. Results and Discussions

The scenarios encountered originally were completely Ricean LOS channels when the absorber-panel was not used. The acquired channel transfer matrices for LOS channels were normalized to calculate channel capacities when the transmitter was fixed at position B whilst the receiver was placed at positions I, D, G, F and H respectively, as shown in Fig.1. The calculated mean capacity C_0, mean root mean square delay spread σ_τ and mean Ricean *K* factor for LOS scenarios at the five receiving positions are tabulated in Table I.

Later, we performed obstructed LOS channel measurements by placing the absorber-panel at the centre between the transmitter and the receiver when the receiver was located at positions I, D and G, respectively. Correspondingly, the calculated mean capacity C_1, mean RMS delay spread σ_τ and mean Ricean *K* factor for the obstructed conditions at the three receiving positions are given in Table II. Obviously, the use of the absorber-panel results in a smaller value of Ricean *K* factor as compared to that of the corresponding LOS case at the same position as given in Table I.

Fig.2 shows the plots of the complementary cumulative distribution functions (CCDF) of channel capacity for both the LOS and OLOS cases when the receiver was located at positions I, D and G. The capacity of an ideal uncorrelated 4×4 MIMO channel, where the entries of the channel matrix are independent and identically distributed (i.i.d) complex Gaussian variables with zero-mean and unit variance [1], is also included in Fig.2 for

comparison. Note that the first normalization scheme was used to calculate the capacity C_0 in Table I, C_1 in Table II and the CCDF of capacity plotted in Fig.2.

The results in Table I for LOS scenarios reveal that the channel capacity, at the five receiving positions, increases whilst the value of *K* factor decreases. This is consistent with the theoretical analysis in [4,5]: in Ricean channels, a larger value of *K* factor degrades the achievable MIMO capacity. In addition, *K* factor decreases with the increase in the separation between the transmitter and receiver. Amongst the five receiving positions, the lowest capacity of 15.91 bits/s/Hz was calculated when the receiver was located at position I, where the largest *K* factor of 7.44 dB was observed. The largest MIMO capacity of 19.08 bits/s/Hz was obtained at receiving position F, where the smallest Ricean factor equal to 3.76 dB was estimated.

The CCDF plots in Fig.2 show that, except at position G, the obtained MIMO capacity under obstructed LOS conditions, is higher than the capacity calculated under LOS conditions at positions I and D, respectively, for the same receive SNR level. This implies that, for the same receive SNR level, for a LOS MIMO channel, the capacity can be improved if the LOS path is obstructed. The reason for this could be due to the presence of a stronger LOS component which results in a higher spatial correlation between MIMO subchannels, which in turn is detrimental for achieving higher capacity. Fig.2 also reveals that the achievable MIMO capacity for both LOS and OLOS conditions is less than that of the uncorrelated i.i.d channel.

Comparing the LOS data in Table I with the OLOS data in Table II at the same receiving positions, it was found that, besides the difference in *K* values, the variations in capacity always follow the corresponding deviations in the value of mean RMS delay spread of the channels. Generally, the obstructions of LOS path result in smaller values of *K* factor and larger values of RMS delay spread. Consequently, a higher capacity is achieved. At

position I, the mean capacity increases from 15.91 bits/s/Hz for LOS case to 19.80 bits/s/Hz for OLOS case and correspondingly an increase of 9.89 ns in delay spread and a decrease *K* value of 3.66 dB was observed. At position D, the mean capacity increases by 14% from LOS case to OLOS scenario, followed by a 28.6% increase in the values of RMS delay spread and a 35% decrease in the value of *K* factor. However, at position G, the mean capacity for LOS case decreases by about 0.56 bits/s/Hz from its OLOS case, followed by a decrease of 0.9 ns in RMS delay spread and an increase of 0.49 dB in Ricean *K* value. The reason for this special case will be considered later.

Using the second normalization scheme, we recalculated the capacity for obstructed LOS cases at the three receiving positions to account for the path loss effect due to absorber-panel. The recalculated capacity, C_2, is included in Table II. Comparing C_2 with the respective C_0 in Table I, capacity deviation of 26.3%, 18.1% and 3.2% occurs at the three receiving positions, respectively. Obviously, this decrease in capacity is due to the path loss introduced by the use of the absorber-panel. The reason for different deviation rates at three receiving position is as follows: according to the Fresnel formulation of Huygens' principle [8], different Fresnel zones were obstructed by the absorber-panel which has fixed dimensions. Thus, different amounts of LOS power were obstructed at the three receiving positions. The radius of the n^{th} Fresnel zone, denoted by r_n, is a function of n, λ and the distance, d_1, from the transmitter and the distance, d_2, from the receiver, given by $r_n = \sqrt{n\lambda d_1 d_2 / (d_1 + d_2)}$ [8]. When the receiver was located at position I, which had a separation of 3 m from position B, the first three Fresnel zones could be obstructed when the absorber-panel was used. When the receiver was located at position D, which had a separation of 5 m from position B, the first two Fresnel zones could be obstructed. However, when the receiver was located at position G, which had a separation of 9.5 m from position B, even the first Fresnel zone, which has a radius of 0.55 m, could not completely be

obstructed as dictated by the fixed dimensions of the absorber-panel. The obstruction of LOS power is evident from the measured power delay profile plotted in Fig.3 for the three receiving positions. The combination plot given in Fig.3 is obtained by off-setting the time axis of the power delay profile at positions D (150 ns) and I (300 ns). As can be seen from Fig.3, at positions D and I, the absorber-panel indeed obstructed most of the LOS power. This is further verified by the decrease in the values of K factor for the OLOS cases compared with their LOS cases. However, at position G, it is clear from Fig.3 that the same absorber-panel has not obstructed the LOS power. In contrast, some scattering could have been obstructed. This is the reason that the OLOS capacity C_1 at position G is slightly smaller than its LOS capacity C_0.

IV. Comparison with Theory

Fig. 4 presents the comparison for 4×4 MIMO ergodic capacity for SNR of 20 dB between measured results and the theoretical predictions. The theoretical results were taken from [5]. In the plot, the best fitted solid line, for measurement data, is based on a least square sense. As can be seen, the trend that the capacity decreases with the increase in the values of Ricean K factor is consistent between the measurements and the theoretical results. However, the rate of decrease of the measured results is much faster than that predicted by the theory [5]. This may be attributable to the difference in the construction of the channel matrix H in [5], where, H is a combination of a pure i.i.d scattered part H^{sc} and a specular part H^{sp} with all unit entries. On the other hand, for practical Ricean channels, the scattered matrix may have certain correlation and the specular part may also contain non-unity entries.

V. Conclusions

The effect of LOS component on the achievable Ricean MIMO capacity in an indoor environment was studied experimentally. Our results demonstrate the effect of the

contribution of LOS component on indoor MIMO capacity when using an absorber-panel to obstruct the different Fresnel zones. Further, comparison with theory demonstrates that the channel capacity consistency has a decreasing trend with the increase in Ricean *K* factor. Our results also reveal that the channels, which have larger values of root mean square delay spread, can achieve higher MIMO capacities. In addition, the measured MIMO capacities are all less than that of the ideal uncorrelated i.i.d channels.

Acknowledgement:

The project is funded by the Australian Research Council through an ARC linkage grant with Singtel Optus Pty Ltd as the industry partner.

References

[1] G. J. Foschini and M. J. Gans, "On limits of wireless communications in a fading environment," *Wireless Personal Commun.,*, vol. 6, pp. 311-335, Mar.1998.

[2] M. Herdin, H. Ozcelik, H. Hofstetter, and E. Bonek, "Variation of measured indoor MIMO capacity with receive direction and position at 5.2 GHz," *IEE Electron. Lett.*, vol. 38, pp. 1283 - 1285, Oct. 2002.

[3] J. W. Wallace and M. A. Jensen, "Modeling the indoor MIMO wireless channel," *IEEE Trans. AP.*, vol. 50, pp. 591 -599, May 2002.

[4] M. A. Khalighi, J.-M. Brossier, G. Jourdain, and K. Raoof, "On capacity of Rician MIMO channels," in proc. IEEE Int. Symp. on Personal, Indoor and Mobile Radio Communications, PIMRC 2001, vol. 1, pp. A-150 -A-154, 2001.

[5] G. Lebrun, M. Faulkner, M. Shafi, and P. J. Smith, "MIMO Ricean Channel Capacity," in proc. 2004 IEEE Int. Conf. on Commun., ICC 2004, vol. 5, pp. 2939-2943.

[6] V. Erceg, P. Soma, D. S. Baum, and A. J. Paulraj, "Capacity obtained from multiple-input multiple-output channel measurements in fixed wireless environments at 2.5 GHz," in proc. IEEE Int. Conf. on Commun., ICC 2002, vol. 1, pp. 396 -400.

[7] L. J. Greenstein, D. G. Michelson, and V. Erceg, "Moment-method estimation of the Ricean K-factor," *IEEE Commun. Lett.*, vol. 3, pp. 175-176, June 1999.

[8] R. Janaswamy, *Radiowave Propagation and Smart Antenna for Wireless Communications*, 1st ed: Kluwer Academic Publisher, 2001.

Authors' affiliations:

Zhongwei Tang and Ananda S. Mohan

Microwave and Wireless Technology Research Lab,

I&C Group, Faculty of Engineering, University of Technology Sydney

E-mail: zhongwei@eng.uts.edu.au, ananda@eng.uts.edu.au

Table captions:

Table I: Mean MIMO capacity, RMS delay spread σ_τ and K factor for line-of-sight cases.

Table II: Mean MIMO capacity, RMS delay spread σ_τ and K factor for obstructed line-of-sight cases.

Figure captions:

Fig. 1. The floor plan of the classroom.

Fig. 2. CCDF of measured MIMO capacity at SNR=20 dB.

Fig. 3. Measured PDP for LOS and OLOS cases at receiving positions I, D and G.

Fig. 4. Comparison with theoretical results.

Table I:

TX position	**RX position**				
B	**I**	**D**	**G**	**H**	**F**
C_0	*15.91*	17.26	*18.92*	*18.99*	*19.08*
K [dB]	7.44	6.05	4.25	4.10	3.76
σ_τ [ns]	19.18	20.97	21.41	24.35	22.64

Table II:

TX position	**RX position**		
B	**I**	**D**	**G**
C_1	*19.80*	19.64	*18.36*
K [dB]	3.78	3.93	4.74
σ_τ [ns]	29.07	26.96	20.51
C_2	*11.74*	14.16	*18.27*

Figure 1

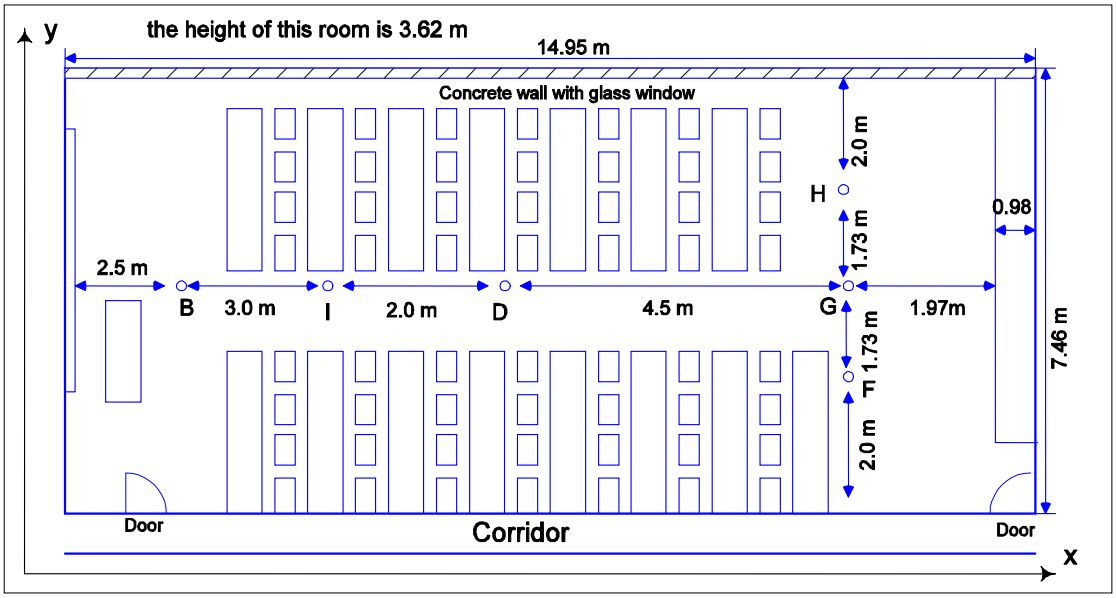
y
the height of this room is 3.62 m
14.95 m
Concrete wall with glass window
2.0 m
H
1.73 m
0.98
2.5 m
B
3.0 m
I
2.0 m
D
4.5 m
G
1.97m
1.73 m
F
2.0 m
7.46 m
Door
Corridor
Door
x

Figure 2

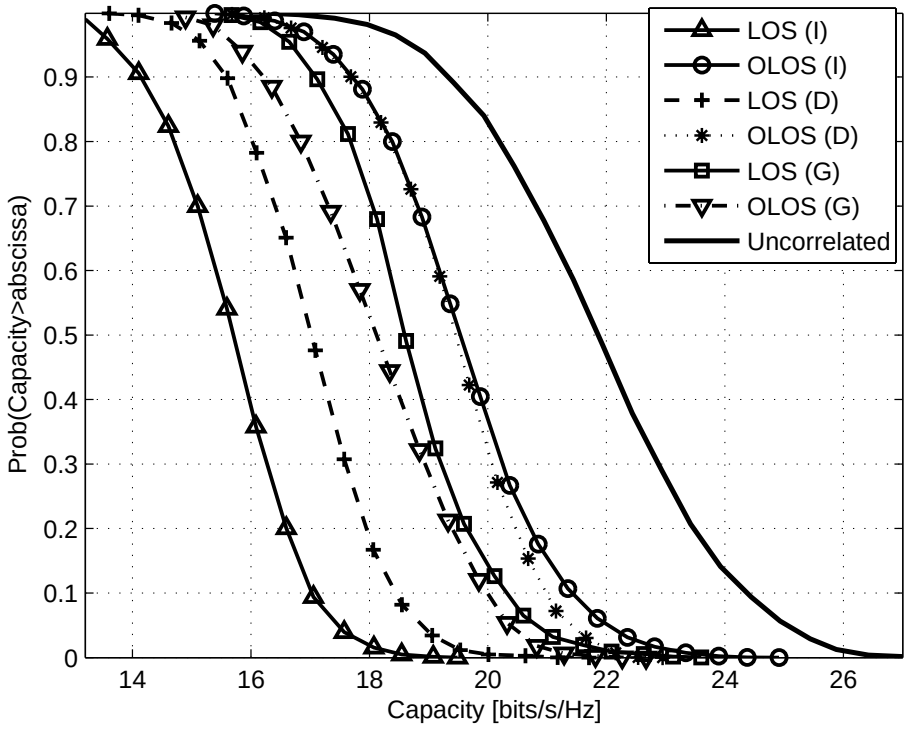
LOS (I)
OLOS (I)
LOS (D)
OLOS (D)
LOS (G)
OLOS (G)
Uncorrelated
Prob(Capacity>abscissa)
Capacity [bits/s/Hz]
0
0.1
0.2
0.3
0.4
0.5
0.6
0.7
0.8
0.9
14
16
18
20
22
24
26

Figure 3

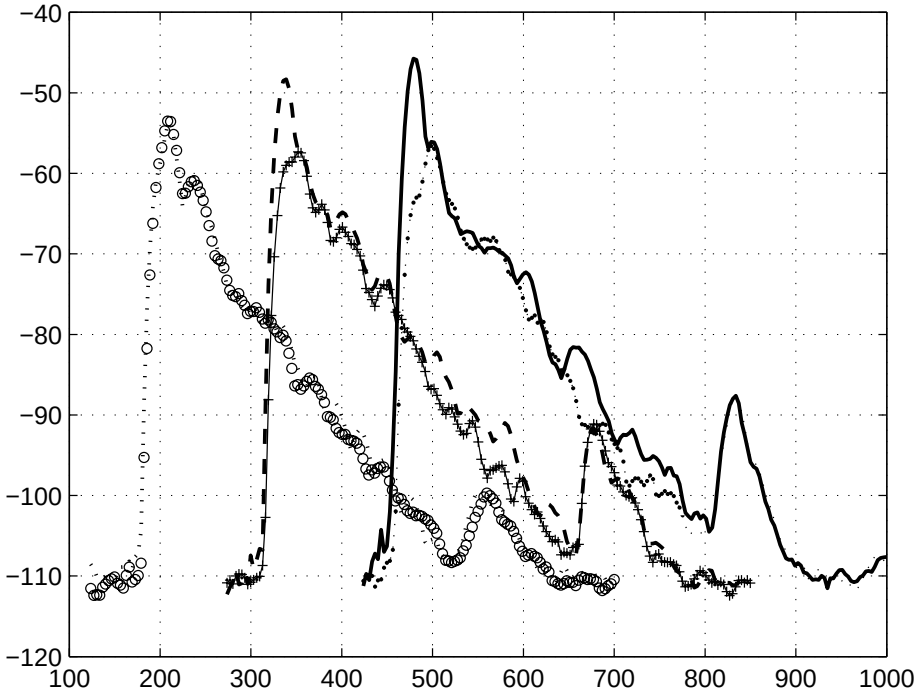
−40
−50
−60
−70
−80
−90
−100
−110
−120
100
200
300
400
500
600
700
800
900
1000

Figure 4

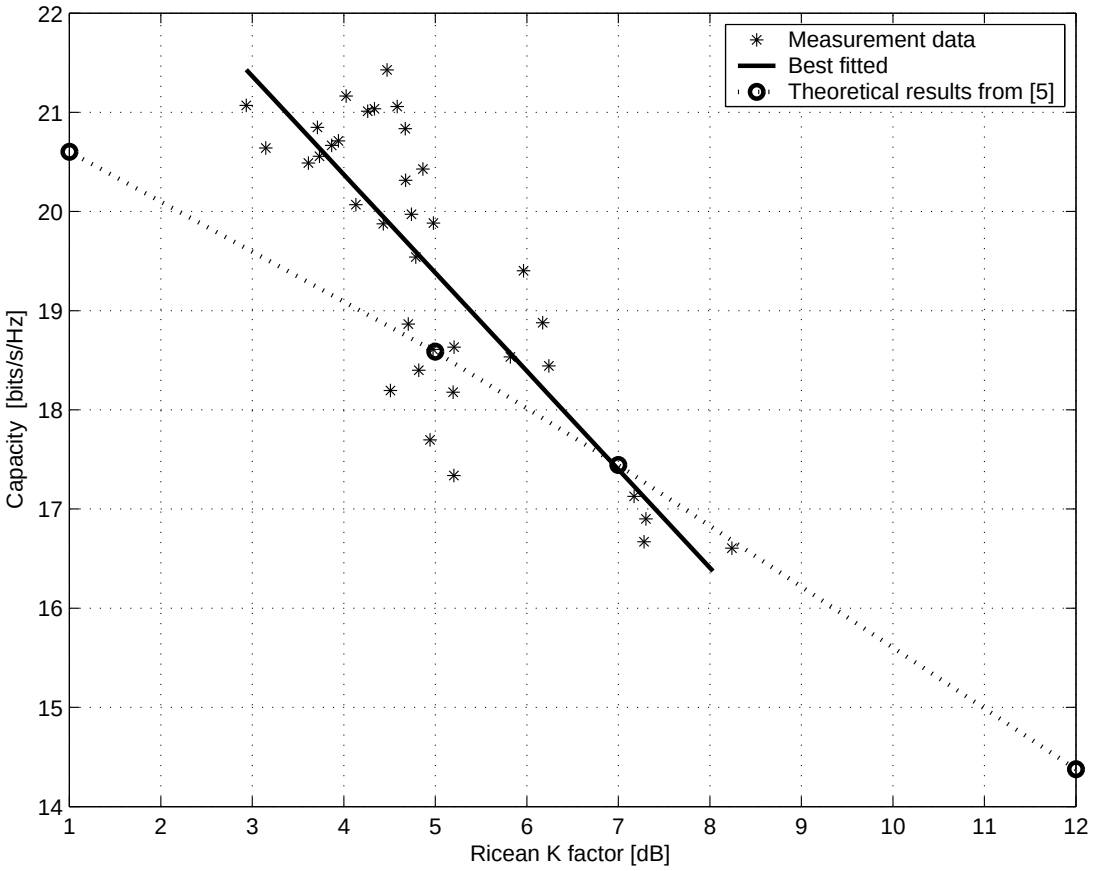
Measurement data
Best fitted
Theoretical results from [5]
Capacity [bits/s/Hz]
Ricean K factor [dB]
22
21
20
19
18
17
16
15
14
1
2
3
4
5
6
7
8
9
10
11
12